CGMS-45 JMA-WP-04
V02, JUNE 2017
Prepared by JMA
Agenda Item: II/6
Discussed in WGII

Validation of Himawari-9/AHI Level-1 and -2 data during In-orbit Test

The Himawari-9 geostationary meteorological satellite of the Japan Meteorological Agency (JMA) was launched on 2 November 2016 and put into in-orbit standby as backup for Himawari-8 on 10 March 2017. Himawari-9 features the Advanced Himawari Imager (AHI), which is identical to the AHI on board Himawari-8. As accurate image navigation and radiometric calibration are essential in leveraging the imager's potential, Himawari-9/AHI Level-1 and -2 data performance was validated during the satellite's period of in-orbit test (IOT).

Image navigation and registration errors determined from observation during the IOT phase were in the same order as those of Himawari-8/AHI. The validation results for Himawari-9/AHI calibration generally show close correspondence to those for Himawari-8/AHI, although larger biases are seen in several bands. Further evaluation will be performed in the near future.

Quality assessment of Atmospheric Motion Vectors (AMVs) and Clear Sky Radiance (CSR) for the AHIs on board Himawari-8 and -9 was also carried out. The rawinsonde statistics for AMVs were similar for both satellites. In regard to CSR, the first-guess (FG) departure statistics for B08 and B10 were similar for both satellites, although the B09 FG departure for Himawari-9 was 0.2 K greater.

Action/Recommendation proposed: none

Validation of Himawari-9/AHI Level-1 and -2 data during its In-Orbit Test

1 INTRODUCTION

The Japan Meteorological Agency's new-generation Himawari-8 geostationary meteorological satellite began operation in July 2015 after in-orbit test (IOT) and checking of the overall system. The identically configured Himawari-9 was launched on 2 November 2016, and was put into in-orbit standby as backup for Himawari-8 on 10 March 2017 after IOT. This set-up will help to ensure the stability of satellite observation for the East Asia and Western Pacific regions for 15 years. Himawari-8 and -9 feature new Advanced Himawari Imager units (referred to here as AHI-8 and AHI-9) with a sensor configuration similar to that of the Advanced Baseline Imager (ABI) on the GOES-16 satellite (Table 1-1).

The AHI conducts observation to produce full-disk imagery every 10 minutes. During the 10-minute timeline of such observation, the AHI scans the Japan and Target Area observations every 2.5 minutes and two Landmark Area observations at 30-second intervals. One of the Landmark Area observations can be applied to the moon based on advance prediction of lunar positioning. The large amount of AHI lunar observation data produced (in comparison to that of heritage imagers on board geostationary satellites) is expected to be useful in validating AHI calibration trends.

Section 2 of this paper provides general information on the Himawari-8/9 AHI, Section 3 covers the image navigation and registration (INR) performance of Himawari-9, Section 4 details the results of validation regarding radiometric calibration, Section 5 outlines quality assessment of AMVs and CSRs for Himawari-9, and Section 6 provides the conclusion.

Table 1-1 General information on Himawari-8/-9 AHI, GOES-16 ABI and MTSAT-2 IMAGER

	Himawari-8/-9	GOES-16	MTSAT-2
Radiometer	AHI	ABI	IMAGER
Bands	16 VIS:3, NIR:3, IR:10	16 VIS: 2, NIR: 4, IR:10	5 VIS:1, IR:4
Spatial resolution at SSP	0.5 km, 1 km, 2 km	0.5 km, 1 km, 2 km	1km, 4 km
Full disk observation	Every 10 minutes	Every 15 minutes (planned)	Hourly
Scan pattern	West to East 23 scans cover full disk	West to East 22 scans cover full disk	Both directions from West and East. Around 1400 scans cover full disk
Orbit determination	Ranging	Ranging + GPS	Ranging
Attitude determination	Star tracker + Rate sensor and so forth	Star tracker + Rate sensor and so forth	Sun sensor + Earth sensor
Navigation correction	Landmark analysis	Star sensing	Landmark analysis

2 AHI BASICS

Table 2-1 and Figure 2-1 show observing band configuration and the spectral response functions (SRFs) of AHI-8 and -9, respectively. The AHIs are manufactured by the ABI vendor, but feature the 0.51-μm band rather than the 1.38-μm band. True-color imagery is derived by composing the three visible bands (i.e., blue: 0.47 μm; green: 0.51 μm; red: 0.64 μm). SRF data are provided on JMA's Meteorological Satellite Center (MSC) website at:
http://www.data.jma.go.jp/mscweb/en/himawari89/space_segment/spsg_ahi.html

Table 2-1 Band configuration of AHI-8/-9 and IMAGER on MTSAT-2. Wlen is the central wavelength [μm], and Sres represents spatial resolution at the SSP [km].

		B01	B02	B03	B04	B05	B06	B07	B08	B09	B10	B11	B12	B13	B14	B15	B16
Himawari-8/-9	Wlen	0.47	0.51	0.64	0.86	1.6	2.3	3.9	6.2	6.9	7.3	8.6	9.6	10.4	11.2	12.4	13.3
	Sres	1	1	0.5	1	2	2	2	2	2	2	2	2	2	2	2	2
MTSAT-2	Wlen			0.68				3.7	6.8					10.8		12.0	
	Sres			1				4	4					4		4	

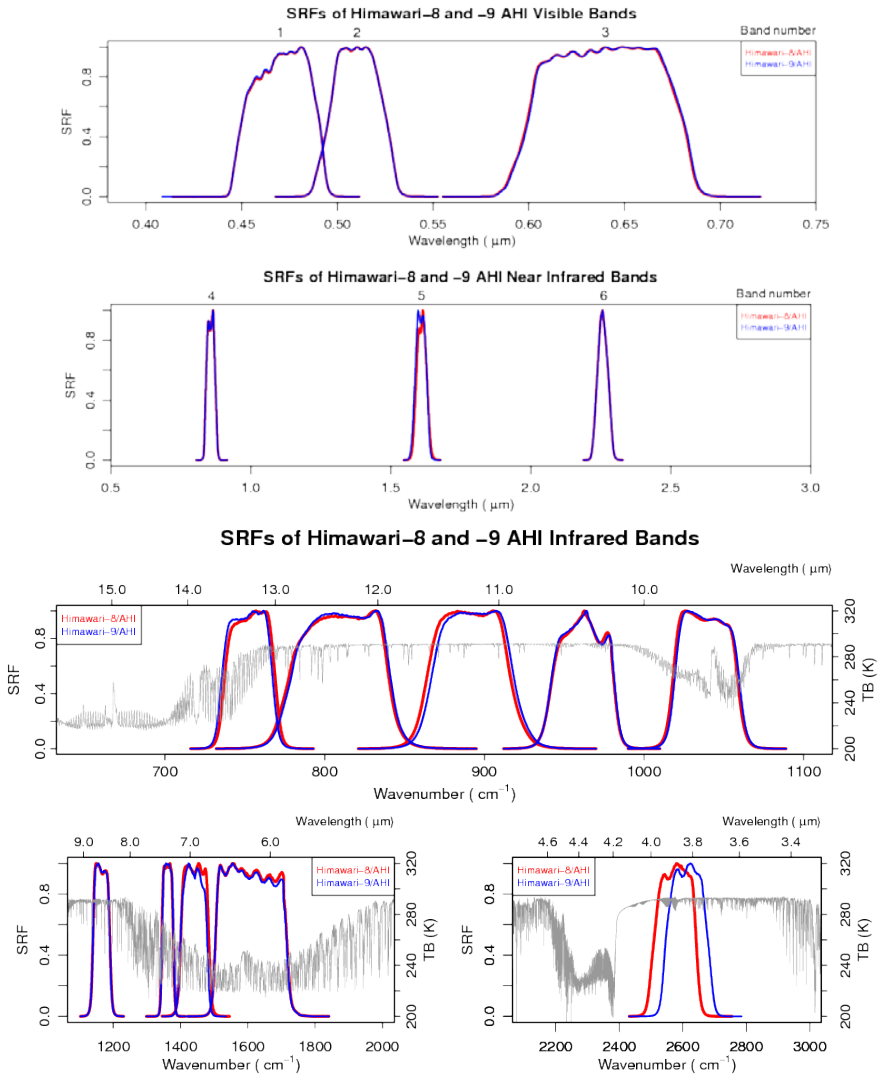

Figure 2-1 Spectral response functions of AHI-8 (red) and -9 (blue)

3 IMAGE NAVIGATION AND REGISTRATION

The INR process for AHI-9 is identical to that of AHI-8, which is based on information from star trackers, inertia reference units and angular rate sensors on board the satellite. JMA validated the INR performance of AHI-9 during in-orbit test using the landmark and band-to-band co-registration analysis methods. The former involves comparing coastlines recognized in observation data with those on reference maps to derive absolute INR errors. The latter is similar, but involves comparison of cloud patterns as well as coastlines in target-band observation data with those in the reference band (e.g., B13) for estimation of band-to-band relative INR errors in each band with the reference band.

Figure 3-1 shows landmark analysis results for B13 Himawari Standard Data (i.e., Level-1 data after rectification). The estimated magnitudes of image navigation errors are around 7.37 μrad (0.26 km at the sub-satellite point (SSP)) and 10.5 μrad (0.38 km at the SSP) at 00:00 and 12:00 UTC, respectively.

Table 3-1 shows diurnally averaged INR errors based on landmark analysis for several bands on the same day. The results indicate that AHI-9 image navigation performance is comparable to that of AHI-8. However, several significant navigation errors are observed daily in AHI-9 observation imagery (figures not shown). The root cause of this is currently being researched by the satellite vendor.

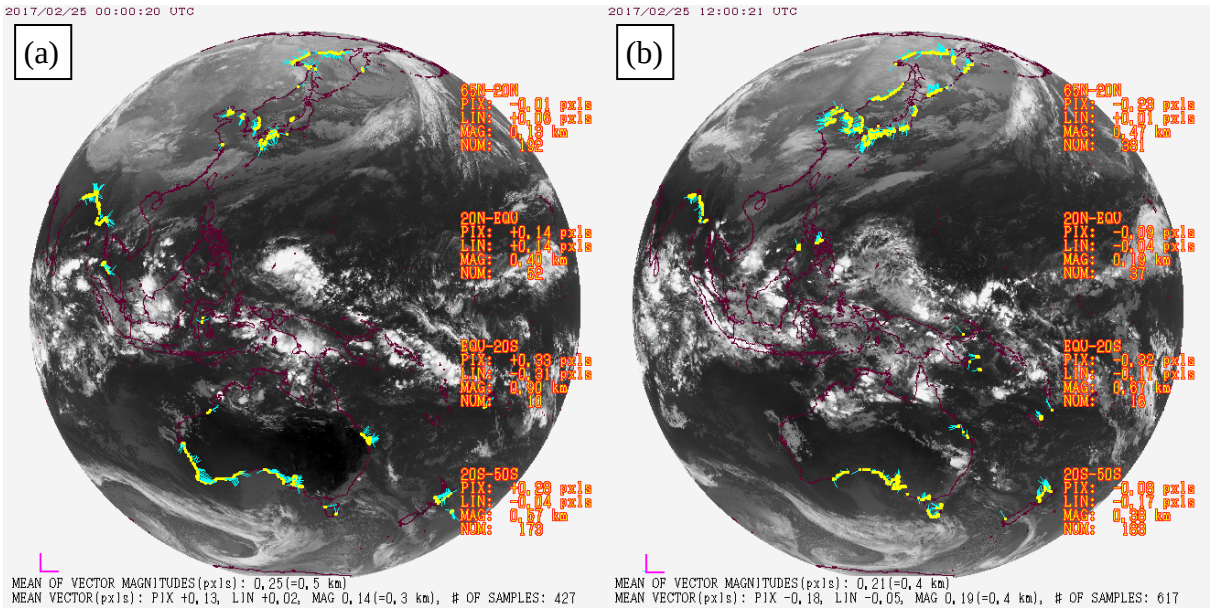

Figure 3-1 (a) AHI-9 Landmark analysis results for B13 at 00:00 on UTC 25 Feb. 2017 (b) As per (a), but for 12:00 UTC. Yellow circles show reference points used to compute misplacement. Blue segments connected with the yellow circles indicate directions and magnitudes of misplacement at each reference point. The short magenta segment (bottom-left) represents the unit length of magnitude for misplacement (i.e., 56 μrad, or one pixel for infrared bands, for which the horizontal resolution is 2 km at the SSP).

Table 3-1 Diurnally averaged INR errors based on landmark analysis for several AHI-9 bands on 25 Feb. 2017

	B01	B07	B13	B15
East-West (μ Rad)	0.026	-4.145	-3.309	-3.329
North-South (μ Rad)	-3.461	-0.241	1.287	3.134
Bias Magnitude(μ Rad)	9.100	10.313	9.633	10.531

Band-to-band co-registration correction has been applied since the start of AHI-9 in-orbit test. Figure 3-2 shows the co-registration analysis results for B07 and B15 with respect to B13. The magnitude of the misplacement is below 1.1 μrad (0.04 km at the SSP), and the co-registration performance of other bands is comparable.

Table 3-2 shows diurnally averaged band-to-band co-registration errors for all bands based on observation data for 25 February 2017. As with image navigation performance, AHI-9 co-registration performance is comparable to that of AHI-8.

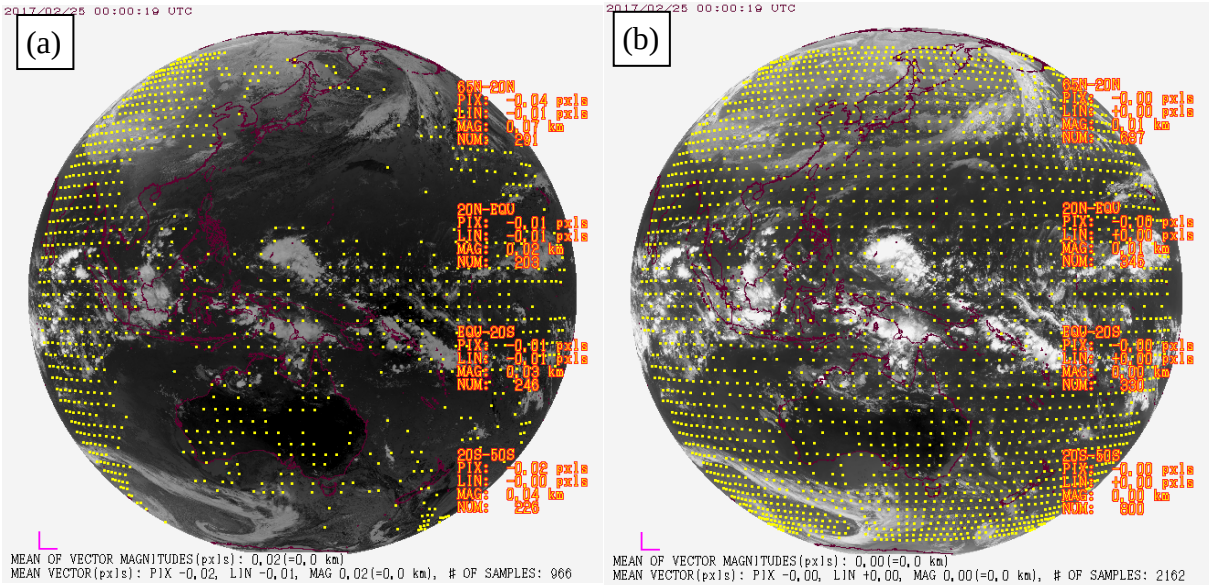

Figure 3-2 (a) band-to-band co-registration analysis for B07 in comparison with B13 at 00:00 UTC on 25 Feb. 2017, and (b) the same for B15. Circles and segments show reference points and their magnitudes as in Figure 3-1.

Table 3-2 Diurnally averaged band-to-band co-registration errors for all bands with respect to B13 for 25 February 2017

Band number	B01	B02	B03	B04	B05
Bias Magnitude(μ Rad)	0.990	1.014	1.220	1.553	1.313

Band number	B06	B07	B08	B09	B10
Bias Magnitude(μ Rad)	1.327	0.817	0.289	0.444	0.501

Band number	B11	B12	B14	B15	B16
Bias Magnitude(μ Rad)	0.576	0.519	0.579	0.223	0.286

4 CALIBRATION

For calibration of observation data, the AHI has a solar diffuser serving as a solar calibration target for visible and near-infrared bands (i.e., B01-06) and a blackbody serving as an internal calibration target for 10 infrared bands (i.e., B07-16). JMA has been validating AHI-8 data quality based on the GEO-LEO technique (involving inter-calibration and vicarious calibration (Okuyama et al. 2015)), lunar calibration and other approaches. These calibration and validation methods have been developed via international collaboration with NOAA (Wu 2016), EUMETSAT and GSICS member agencies in addition to collaborative research with the Atmosphere and Ocean Research Institute at the University of Tokyo. This article reports on AHI-9 validation using some of these approaches. Tables 4-1 and 4-2 summarize the results for all 16 AHI-8 and -9 bands.

For visible and near-infrared bands (Table 4-1), radiances were validated based on 1) comparison with top-of-atmosphere radiance computed via radiative transfer simulation (vicarious calibration) and 2) a ray-matching approach with reference to S-NPP/VIIRS. Estimated radiance biases of AHI-9 from the vicarious calibration approach were +2.94 and -5.48% for B01 and B06, but the biases for other bands were less than +/- 2.0%. The ray-matching approach provided results consistent with those of the vicarious calibration approach for B01 and B06. Infrared inter-calibration (Table 4-2) with reference to hyperspectral infrared sounders such as Metop-A/IASI showed that brightness temperature biases for AHI-9 are in the same order as those validated for AHI-8 (less than 0.25 K for standard scenes (i.e., simulated brightness temperature for the US standard atmosphere)) in all 10 infrared bands.

The frequent full-disk observation conducted by AHI-8 and -9 (with a repeat cycle of 10-minutes) also enables application of the highly useful GEO-GEO comparison approach. Although the GEO-GEO approach is a relative comparison method without accurate reference sensor such as IASI and VIIRS, the huge amounts of collocated data enable identification of calibration issues (such as diurnal variation of biases, stray light and banding) on a real-time basis. In this study, AHI-8 and -9 Himawari Standard Data from the same observation time and the same band were averaged for areas of 19 x 19 pixels and compared in terms of scaled radiance (for visible and near-infrared bands) and brightness temperature (for infrared bands).

For verification of consistency between the GEO-LEO and GEO-GEO approaches mentioned above, the relative differences between AHI-8 and -9 of the GEO-LEO approaches are shown at the bottom of Tables 4-1 and 4-2 along with GEO-GEO approach results. Ratios of AHI-9/AHI-8 are shown for visible and near-infrared bands in Table 4-1, and differences in biases for AHI-9 minus AHI-8 in standard scenes for infrared bands are shown in Table 4-2. For infrared bands, the effects of spectral response function difference were removed from GEO-GEO results using AHI-8 and -9 pseudo data from Metop-A/IASI for a particular scene (14 January 2015, latitude within 30 deg., longitude within 80 deg. from the Himawari-8/-9 sub-satellite point (140.7°E, 0.0°N)). Close correspondence between the comparison results for each approach is observed in Figure 4-1. This validation approach offers a promising solution for the generation of a new inter-calibration product combining GEO-LEO and GEO-GEO comparison results to account for diurnal calibration variations.

Table 4-1 Estimated observation biases of AHI-8 and -9 for visible and near-infrared bands (in scaled radiance [%] for vicarious calibration and GEO-GEO approaches, and in reflectance [%] for ray-matching approach). Observation data for the period from 14 to 28 February 2017 for AHI-8 and AHI-9 are used in these approaches. AHI-9 calibration coefficients other than offset terms were determined based on pre-launch ground test whereas AHI-8 calibration slopes were updated on 8 June 2015 to reflect the solar diffuser viewing data collected in orbit.

		B01	B02	B03	B04	B05	B06
AHI-8 [%]	Vicarious cal.	-1.61	-2.55	+0.71	+1.62	+4.61	-3.02
	Ray-matching	-2.50	+1.13	+1.92	+0.62	+6.59	-4.50
AHI-9 [%]	Vicarious cal.	+2.94	-1.85	-1.82	+0.01	-1.15	-5.48
	Ray-matching	+3.15	+2.83	+0.39	-0.031	+0.59	-6.22
(AHI-9)/(AHI-8) [%]	Vicarious cal.	+4.63	+0.72	-2.51	-1.58	-5.51	-2.54
	Ray-matching	+5.79	+1.68	-1.50	-0.65	-5.63	-1.80
	GEO-GEO	+4.75	+1.02	-2.22	-1.45	-5.79	-2.00

Table 4-2 Estimated observation biases of AHI-8 and -9 in brightness temperature [K] for infrared bands. Observation data for the period from 14 to 28 February 2017 for AHI-8 and AHI-9 are used in these approaches. Only results from nighttime Metop-A/IASI (10 - 14 UTC) are shown.

		B07	B08	B09	B10	B11	B12	B13	B14	B15	B16
AHI-8 [K]	Metop-A/IASI	-0.13	-0.24	-0.25	-0.14	-0.09	-0.25	-0.01	0.00	-0.08	+0.05
AHI-9 [K]	Metop-A/IASI	-0.08	-0.25	-0.04	-0.15	-0.12	-0.20	-0.10	-0.11	-0.13	-0.23
(AHI-9)-(AHI-8)[K]	Metop-A/IASI	+0.05	-0.01	+0.21	-0.01	-0.03	+0.05	-0.09	-0.11	-0.04	-0.28
	GEO-GEO	+0.05	-0.03	+0.19	-0.02	-0.02	+0.06	-0.05	-0.08	-0.02	-0.25

(a) (b)

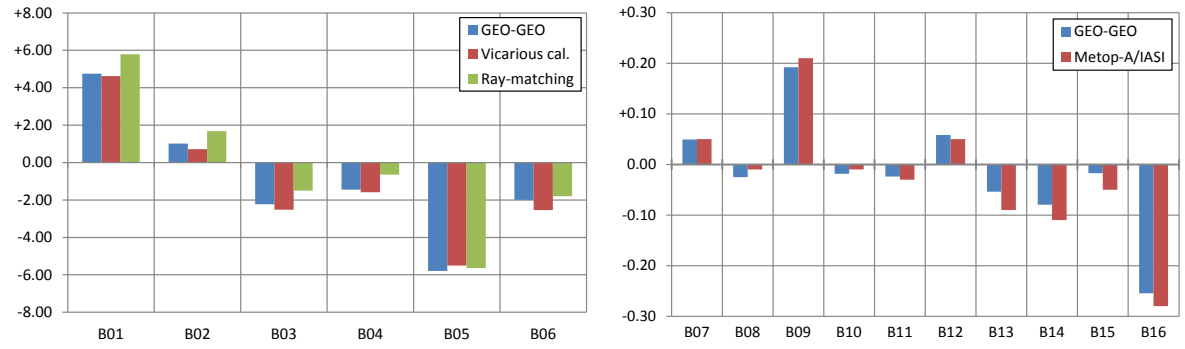

Figure 4-1 Consistency of different approaches in terms of (a) ratios of (AHI-9)/(AHI-8) [%] for visible and near-infrared bands, and (b) differences in AHI-9 and AHI-8 biases [K] for infrared bands

5 LEVEL-2 PRODUCTS

Quality assessment of AMVs (Atmospheric Motion Vectors) and CSR (Clear Sky Radiance) in the Himawari-9 IOT phase showed consistency with products from the Himawari-8 IOT phase.

5.1 AMV

Rawinsonde statistics for Himawari-8 and -9 AMVs were assessed for the period from 1st to 26th February 2017. The Mean Vector Difference (MVD), RMS Vector Difference (RMSVD) and wind speed bias (BIAS) exhibited improvement, but variations between Himawari-8 and -9 were small. The method, reporting period and filters are detailed below.

Rawinsonde comparison statistics
Method: Comparison of rawinsonde wind data with AMV winds within a 150-km radius of a RAOB site
Reporting period: 1st – 26th February 2017
Filters: VERT. DIST. (> = 700 hPa) < 50 (hPa)
VERT. DIST. (< 700 hPa) < 35 (hPa)
QUALITY >= 85
0.5 * 0.5 deg. latitude/longitude grid point data
SPEED DIFF. < 30 (m/s) – DIRECTION DIFF. < 90 (deg)

The statistics for B03, B08, B09, B10 and B13 are shown in Tables 5-1 to 5-5. Red and blue represent improvement and degradation, respectively.

Table 5-1 VIS (B03) rawinsonde statistics for Himawari-8 (a) and Himawari-9 (b)

(a)

Satellite in use : Himawari-8
Selected channel : B03 (0.64 um)
Target Type : cloudy

	ALL REGIONS	NH EX-TROP	TROP	SH EX-TROP
ALL LEVEL				
MVD	4.18	4.45	4.00	4.09
RMSVD	5.07	5.50	4.76	4.90
BIAS	-0.37	-0.49	-0.32	-0.19
SPD	15.80	20.98	12.26	14.60
NCMV	388324	102042	166196	120086
NC	21117	8013	11014	2090
HIGH LEVEL				
MVD	4.70	5.55	4.34	5.31
RMSVD	5.64	6.75	5.12	6.17
BIAS	-0.83	-0.75	-0.81	-1.32
SPD	20.46	37.00	14.12	25.09
NCMV	81775	13123	51568	17084
NC	10071	2463	6922	686
MEDIUM LEVEL				
MVD	4.15	4.46	3.56	4.35
RMSVD	4.97	5.39	4.12	5.02
BIAS	-0.55	-0.49	-0.63	-0.64
SPD	16.45	21.65	8.13	13.50
NCMV	54138	19798	16718	17622
NC	3114	1833	1069	212
LOW LEVEL				
MVD	3.53	3.71	3.37	3.35
RMSVD	4.29	4.54	4.09	3.95
BIAS	0.28	-0.32	0.91	0.54
SPD	9.62	10.03	9.46	8.76
NCMV	252411	69121	97910	85380
NC	7932	3717	3023	1192

(b)

Satellite in use : Himawari-9
Selected channel : B03 (0.64 um)
Target Type : cloudy

	ALL REGIONS	NH EX-TROP	TROP	SH EX-TROP
ALL LEVEL				
MVD	4.11	4.37	3.92	3.86
RMSVD	4.99	5.37	4.70	4.63
BIAS	-0.34	-0.44	-0.28	-0.18
SPD	16.46	21.49	12.21	15.23
NCMV	310147	81639	135165	93343
NC	19907	8517	9506	1884
HIGH LEVEL				
MVD	4.66	5.42	4.27	5.14
RMSVD	5.59	6.57	5.05	5.93
BIAS	-0.63	-0.38	-0.69	-1.13
SPD	21.24	36.36	13.99	25.40
NCMV	69486	11702	42998	14786
NC	9494	2734	6090	670
MEDIUM LEVEL				
MVD	4.18	4.49	3.64	3.67
RMSVD	4.96	5.32	4.24	4.31
BIAS	-0.48	-0.50	-0.46	-0.38
SPD	16.57	20.88	8.22	12.74
NCMV	42426	15586	13384	13456
NC	3655	2312	1071	272
LOW LEVEL				
MVD	3.29	3.47	3.15	3.00
RMSVD	4.02	4.23	3.89	3.53
BIAS	0.15	-0.45	0.86	0.55
SPD	9.70	10.18	9.39	8.72
NCMV	198235	54351	78783	65101
NC	6758	3471	2345	942

Table 5-2 As per Table 5-1, but for WV (B08) rawinsonde statistics

(a)

Satellite in use : Himawari-8
Selected channel : B08 (6.2 um)
Target Type : cloudy

	ALL REGIONS	NH EX-TROP	TROP	SH EX-TROP
ALL LEVEL				
MVD	4.77	5.64	4.48	5.45
RMSVD	5.69	6.81	5.28	6.40
BIAS	-0.12	-0.12	-0.13	-0.01
SPD	21.99	37.40	17.20	28.33
NCMV	523670	69019	358394	96257
NC	62355	13466	46498	2391
HIGH LEVEL				
MVD	4.77	5.64	4.48	5.45
RMSVD	5.69	6.81	5.28	6.40
BIAS	-0.12	-0.12	-0.13	-0.01
SPD	21.99	37.40	17.20	28.33
NCMV	523670	69019	358394	96257
NC	62355	13466	46498	2391
MEDIUM LEVEL				
MVD	0.00	0.00	0.00	0.00
RMSVD	0.00	0.00	0.00	0.00
BIAS	0.00	0.00	0.00	0.00
SPD	0.00	0.00	0.00	0.00
NCMV	0	0	0	0
NC	0	0	0	0
LOW LEVEL				
MVD	0.00	0.00	0.00	0.00
RMSVD	0.00	0.00	0.00	0.00
BIAS	0.00	0.00	0.00	0.00
SPD	0.00	0.00	0.00	0.00
NCMV	0	0	0	0
NC	0	0	0	0

(b)

Satellite in use : Himawari-9
Selected channel : B08 (6.2 um)
Target Type : cloudy

	ALL REGIONS	NH EX-TROP	TROP	SH EX-TROP
ALL LEVEL				
MVD	4.71	5.48	4.42	5.04
RMSVD	5.60	6.51	5.22	5.88
BIAS	-0.04	0.11	-0.09	0.01
SPD	22.43	36.52	17.03	28.24
NCMV	399883	54134	274609	71140
NC	53319	13599	37689	2031
HIGH LEVEL				
MVD	4.71	5.48	4.42	5.04
RMSVD	5.60	6.51	5.22	5.88
BIAS	-0.04	0.11	-0.09	0.01
SPD	22.43	36.52	17.03	28.24
NCMV	399883	54134	274609	71140
NC	53319	13599	37689	2031
MEDIUM LEVEL				
MVD	0.00	0.00	0.00	0.00
RMSVD	0.00	0.00	0.00	0.00
BIAS	0.00	0.00	0.00	0.00
SPD	0.00	0.00	0.00	0.00
NCMV	0	0	0	0
NC	0	0	0	0
LOW LEVEL				
MVD	0.00	0.00	0.00	0.00
RMSVD	0.00	0.00	0.00	0.00
BIAS	0.00	0.00	0.00	0.00
SPD	0.00	0.00	0.00	0.00
NCMV	0	0	0	0
NC	0	0	0	0

Table 5-3 As per Table 5-1, but for WV (B09) rawinsonde statistics

(a)

Satellite in use : Himawari-8
Selected channel : B09 (6.9 um)
Target Type : cloudy

	ALL REGIONS	NH EX-TROP	TROP	SH EX-TROP
ALL LEVEL				
MVD	4.76	5.45	4.45	5.36
RMSVD	5.68	6.58	5.25	6.29
BIAS	-0.19	-0.14	-0.20	-0.26
SPD	21.95	34.56	16.65	27.38
NCMV	659198	113777	414600	130821
NC	76829	20991	52917	2921
HIGH LEVEL				
MVD	4.74	5.56	4.45	5.37
RMSVD	5.67	6.69	5.25	6.30
BIAS	-0.24	-0.29	-0.22	-0.31
SPD	21.85	36.44	16.78	27.75
NCMV	607361	88249	399721	119391
NC	71598	16901	51899	2798
MEDIUM LEVEL				
MVD	4.94	5.03	4.56	5.22
RMSVD	5.90	6.06	5.18	6.18
BIAS	0.54	0.49	0.69	0.97
SPD	23.35	26.75	10.17	19.00
NCMV	51837	25528	14879	11430
NC	5231	4090	1018	123
LOW LEVEL				
MVD	0.00	0.00	0.00	0.00
RMSVD	0.00	0.00	0.00	0.00
BIAS	0.00	0.00	0.00	0.00
SPD	0.00	0.00	0.00	0.00
NCMV	0	0	0	0
NC	0	0	0	0

(b)

Satellite in use : Himawari-9
Selected channel : B09 (6.9 um)
Target Type : cloudy

	ALL REGIONS	NH EX-TROP	TROP	SH EX-TROP
ALL LEVEL				
MVD	4.67	5.26	4.37	5.03
RMSVD	5.57	6.28	5.16	5.90
BIAS	-0.10	0.09	-0.18	-0.18
SPD	22.36	33.98	16.44	27.16
NCMV	501213	89292	315668	96253
NC	66492	20874	43074	2544
HIGH LEVEL				
MVD	4.66	5.35	4.37	5.05
RMSVD	5.56	6.39	5.17	5.91
BIAS	-0.18	-0.09	-0.21	-0.25
SPD	22.29	35.75	16.59	27.65
NCMV	462325	68851	305128	88346
NC	61361	16859	42084	2418
MEDIUM LEVEL				
MVD	4.80	4.90	4.37	4.76
RMSVD	5.67	5.83	4.96	5.67
BIAS	0.83	0.84	0.78	1.05
SPD	23.11	26.54	9.89	17.69
NCMV	38888	20441	10540	7907
NC	5131	4015	990	126
LOW LEVEL				
MVD	0.00	0.00	0.00	0.00
RMSVD	0.00	0.00	0.00	0.00
BIAS	0.00	0.00	0.00	0.00
SPD	0.00	0.00	0.00	0.00
NCMV	0	0	0	0
NC	0	0	0	0

Table 5-4 As per Table 5-1, but for WV (B10) rawinsonde statistics

(a)

Satellite in use : Himawari-8
Selected channel : B10 (7.3 um)
Target Type : cloudy

	ALL REGIONS	NH EX-TROP	TROP	SH EX-TROP
ALL LEVEL				
MVD	4.72	5.34	4.42	5.25
RMSVD	5.64	6.46	5.22	6.18
BIAS	-0.34	-0.35	-0.33	-0.46
SPD	21.29	32.83	16.07	26.55
NCMV	699461	134100	422484	142877
NC	78492	22451	52852	3189
HIGH LEVEL				
MVD	4.71	5.51	4.42	5.29
RMSVD	5.63	6.64	5.23	6.22
BIAS	-0.37	-0.44	-0.35	-0.49
SPD	21.27	35.81	16.30	27.39
NCMV	602309	86647	396837	118825
NC	70180	16222	51034	2924
MEDIUM LEVEL				
MVD	4.77	4.91	4.27	4.82
RMSVD	5.74	5.97	4.88	5.69
BIAS	-0.05	-0.10	0.12	-0.10
SPD	21.43	25.06	9.59	17.25
NCMV	97152	47453	25647	24052
NC	8312	6229	1818	265
LOW LEVEL				
MVD	0.00	0.00	0.00	0.00
RMSVD	0.00	0.00	0.00	0.00
BIAS	0.00	0.00	0.00	0.00
SPD	0.00	0.00	0.00	0.00
NCMV	0	0	0	0
NC	0	0	0	0

(b)

Satellite in use : Himawari-9
Selected channel : B10 (7.3 um)
Target Type : cloudy

	ALL REGIONS	NH EX-TROP	TROP	SH EX-TROP
ALL LEVEL				
MVD	4.63	5.15	4.33	4.97
RMSVD	5.52	6.16	5.13	5.84
BIAS	-0.23	-0.13	-0.27	-0.30
SPD	21.72	32.03	15.90	26.16
NCMV	536479	105325	324708	106446
NC	69693	23356	43513	2824
HIGH LEVEL				
MVD	4.63	5.30	4.34	5.04
RMSVD	5.52	6.34	5.14	5.89
BIAS	-0.29	-0.25	-0.30	-0.38
SPD	21.75	35.12	16.16	27.21
NCMV	463315	68001	305808	89506
NC	60718	16419	41753	2546
MEDIUM LEVEL				
MVD	4.66	4.80	4.17	4.34
RMSVD	5.53	5.71	4.78	5.30
BIAS	0.20	0.15	0.33	0.42
SPD	21.50	24.71	9.61	16.54
NCMV	73164	37324	18900	16940
NC	8975	6937	1760	278
LOW LEVEL				
MVD	0.00	0.00	0.00	0.00
RMSVD	0.00	0.00	0.00	0.00
BIAS	0.00	0.00	0.00	0.00
SPD	0.00	0.00	0.00	0.00
NCMV	0	0	0	0
NC	0	0	0	0

Table 5-5 As per Table 5-1, but for IR (B13) rawinsonde statistics

(a)

Satellite in use : Himawari-8
Selected channel : B13 (10.4 um)
Target Type : cloudy

	ALL REGIONS	NH EX-TROP	TROP	SH EX-TROP
ALL LEVEL				
MVD	4.50	4.81	4.27	4.68
RMSVD	5.42	5.89	5.04	5.60
BIAS	-0.50	-0.55	-0.48	-0.35
SPD	18.74	24.92	14.12	20.88
NCMV	896671	241477	409601	245593
NC	65879	25896	36343	3640
HIGH LEVEL				
MVD	4.72	5.47	4.37	5.52
RMSVD	5.64	6.61	5.15	6.45
BIAS	-0.63	-0.68	-0.60	-0.76
SPD	20.74	34.76	14.88	28.53
NCMV	383625	55874	246792	80959
NC	45518	11980	31444	2094
MEDIUM LEVEL				
MVD	4.49	4.70	3.89	4.33
RMSVD	5.41	5.71	4.48	5.03
BIAS	-0.35	-0.37	-0.31	-0.21
SPD	18.92	22.58	8.77	15.21
NCMV	139376	61996	39416	37964
NC	9352	6707	2288	357
LOW LEVEL				
MVD	3.64	3.82	3.31	3.30
RMSVD	4.42	4.64	4.02	3.89
BIAS	-0.10	-0.48	0.78	0.32
SPD	10.29	10.74	9.61	9.11
NCMV	373670	123607	123393	126670
NC	11009	7209	2611	1189

(b)

Satellite in use : Himawari-9
Selected channel : B13 (10.4 um)
Target Type : cloudy

	ALL REGIONS	NH EX-TROP	TROP	SH EX-TROP
ALL LEVEL				
MVD	4.40	4.66	4.17	4.35
RMSVD	5.27	5.63	4.93	5.18
BIAS	-0.45	-0.46	-0.45	-0.25
SPD	19.11	24.62	13.94	20.54
NCMV	698182	189953	323496	184733
NC	61003	27533	30287	3183
HIGH LEVEL				
MVD	4.62	5.25	4.28	5.21
RMSVD	5.50	6.27	5.06	6.02
BIAS	-0.53	-0.48	-0.54	-0.67
SPD	21.25	34.11	14.74	28.33
NCMV	309796	48005	196965	64826
NC	40078	12218	26077	1783
MEDIUM LEVEL				
MVD	4.40	4.61	3.73	3.72
RMSVD	5.25	5.51	4.32	4.36
BIAS	-0.31	-0.34	-0.30	0.13
SPD	18.88	21.83	8.58	14.00
NCMV	106660	48194	30475	27991
NC	11169	8494	2223	452
LOW LEVEL				
MVD	3.50	3.67	3.15	3.03
RMSVD	4.23	4.42	3.83	3.57
BIAS	-0.27	-0.59	0.56	0.36
SPD	10.57	11.11	9.47	8.99
NCMV	281726	93754	96056	91916
NC	9756	6821	1987	948

5.2 CSR

The first guess (FG) departure statistics of Himawari-8 and -9 CSR products were evaluated for B08 (6.2 μm), B09 (6.9 μm) and B10 (7.3 μm) in the Himawari-9 IOT phase. The FG value of brightness temperature comes from JMA's Global Spectral Model. Figures 5-1 to 5-3 show FG departure histograms for B08, B9 and B10, respectively. Table 5-6 summarizes FG statistics. Although these statistics represent only single-scene comparisons between Himawari-8 and -9, the values for Himawari-9 (except the mean for B09) are consistent with those of Himawari-8. The Himawari-9 mean for B09 is approximately 0.2 K greater.

Table 5-6 FG departure statistics for Himawari-8 and -9 CSR products (all regions, 02 UTC, 25 February 2017)

Band	Satellite	N	Mean [K]	Sdev [K]
band-08 (6.2um)	Himawari-8	53079	1.40	2.04
	Himawari-9	52940	1.42	2.04
band-09 (6.9um)	Himawari-8	50074	1.07	2.06
	Himawari-9	49795	1.29	2.06
band-10 (7.3um)	Himawari-8	42950	0.15	1.70
	Himawari-9	42465	0.17	1.71

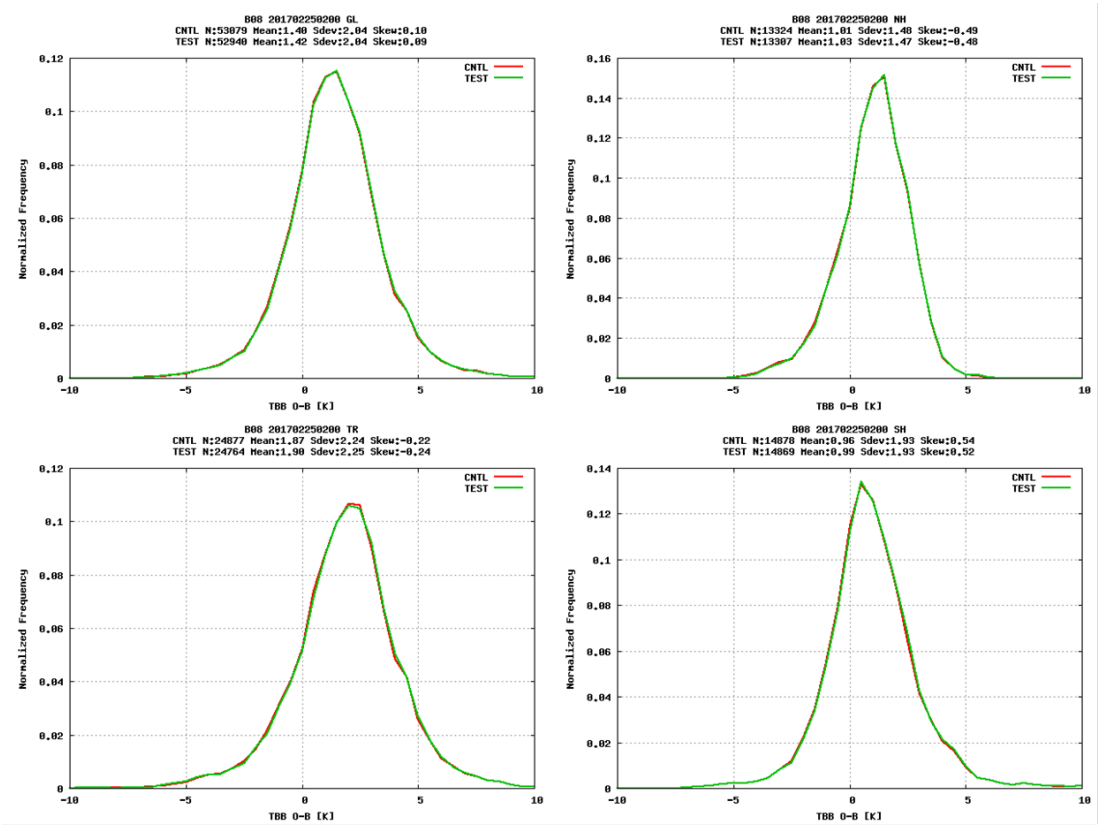

Figure 5-1 FG departure histograms for the B08 (6.2 μm) CSR product in all regions (a), the northern region (b), the tropics (c) and the southern region (d) at 02 UTC on 25 February 2017. CNTL (Himawari-8) and TEST (Himawari-9) are indicated by red and green lines, respectively.

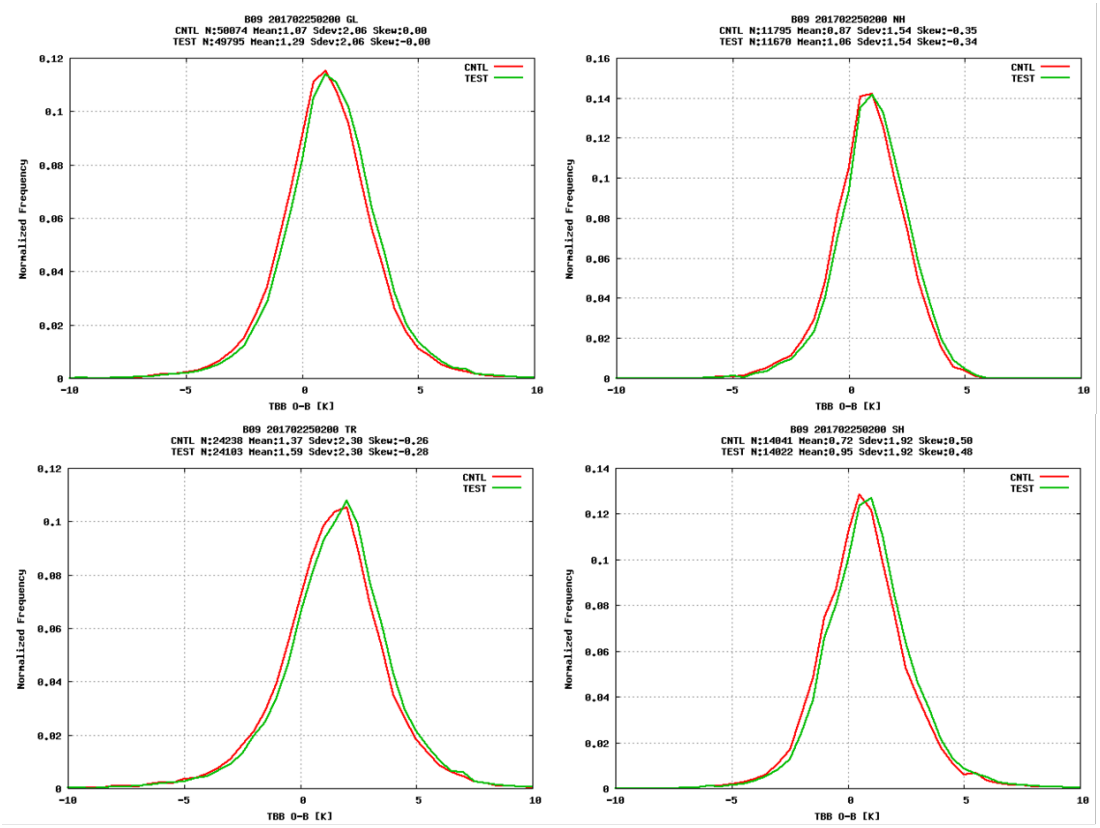

Figure 5-2 As per Figure 5-1, but for histograms of the B09 (6.9 μm) CSR product

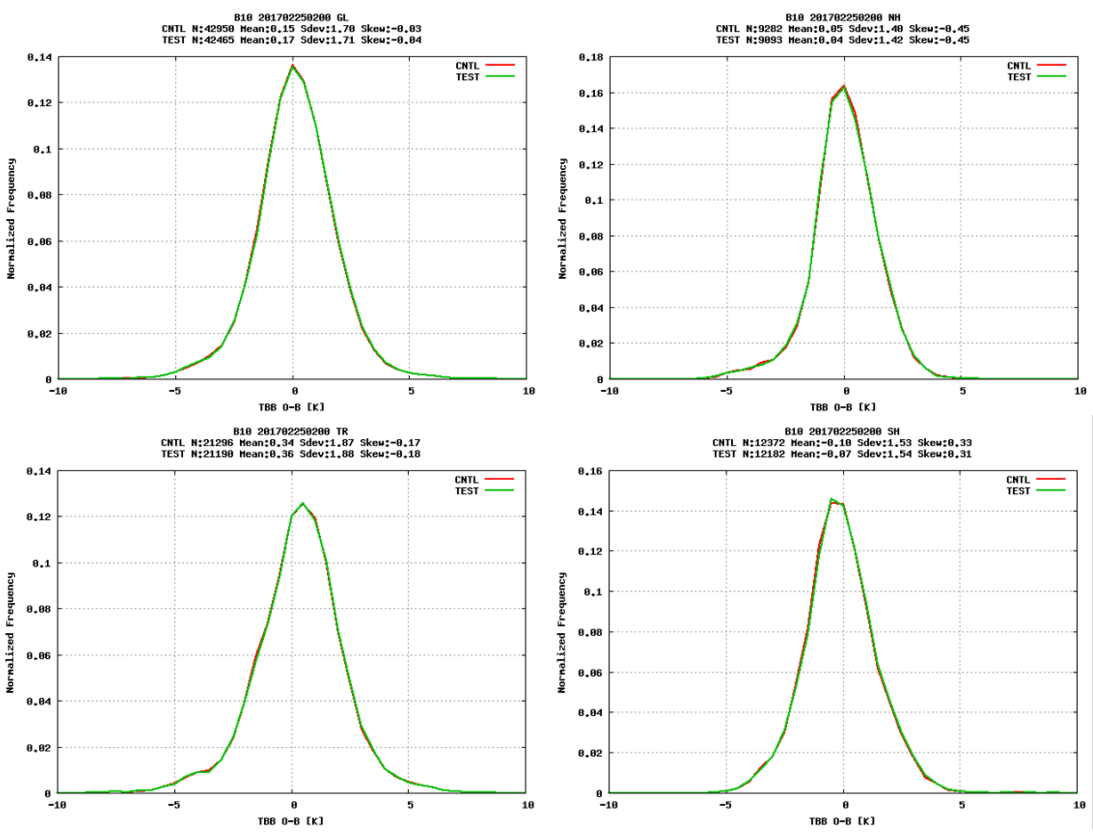

Figure 5-3 As per Figure 5-1, but for histograms of the B10 (7.3 μm) CSR product

6 CONCLUSION

Himawari-9, which features the new-generation AHI visible and infrared imager, was launched on 2 November 2016 and put into in-orbit standby as backup for Himawari-8 on 10 March 2017. This paper reports on the current status of AHI-9's Level-1 and -2 products.

INR errors as determined from observation during the IOT phase are in the same order as those for AHI-8. To validate calibration performance, both GEO-LEO and GEO-GEO approaches were adopted for all 16 bands of AHI-8 and -9. The validation results for AHI-9 calibration generally show close correspondence with those for AHI-8. However, larger biases are seen in several AHI-9 bands (e.g., B01, B06 and B16). One possible reason for the discrepancy in visible and near-infrared bands is that pre-launch calibration slopes were used for AHI-9, whereas coefficients derived from solar diffuser observation are used for AHI-8 bands. In addition to the implementation of new calibration and validation approaches such as a lunar method, calibration trends will also be evaluated further in the near future.

Quality assessment of Himawari-8 and -9 AMVs and CSRs was also carried out. The rawinsonde statistics for AMVs were similar for both satellites. In regard to CSR, the FG departure statistics for B08 and B10 were similar for both satellites, although the B09 FG departure for Himawari-9 was 0.2 K greater.

7 REFERENCES

Okuyama, A., Akiyoshi Andou, Kenji Date, Nobutaka Mori, Hidehiko Murata, Tasuku Tabata, Masaya Takahashi, Ryoko Yoshino, Kotaro Bessho, "Preliminary validation of Himawari-8/AHI navigation and calibration", Proc. SPIE 9607, Earth Observing Systems XX, 96072E (8 September 2015); doi: 10.1117/12.2188978.

Wu, Xiangqian, “Geostationary Operational Environmental Satellite R-Series (GOES-R) launched”, GSICS Quarterly, Volume 10 Number 3, 2016, doi: 10.7289/V5PC30DM.